Hindawi
Advances in Civil Engineering
Volume 2019, Article ID 9898031, 9 pages
https://doi.org/10.1155/2019/9898031

*Research Article*

# Experiment Study of Lateral Unloading Stress Path and Excess Pore Water Pressure on Creep Behavior of Soft Soil

**Wei Huang,[1,2] Kejun Wen,[3] Dongsheng Li,[1,2] Xiaojia Deng,[4] Lin Li,[5] Haifei Jiang,[6] and Farshad Amini[3]**

[1]*School of Civil Engineering and Architecture, Chongqing University of Science and Technology, Chongqing 401331, China*
[2]*Chongqing Key Laboratory of Energy Engineering Mechanics & Disaster Prevention and Mitigation, Chongqing 401331, China*
[3]*Department of Civil and Environmental Engineering, Jackson State University, Jackson, MS 39217, USA*
[4]*School of Civil Engineering, Chongqing University, Chongqing 400045, China*
[5]*Department of Civil and Architectural Engineering, Tennessee State University, Nashville, TN 37209, USA*
[6]*School of Civil Engineering, Chongqing Jiaotong University, Chongqing 400074, China*

Correspondence should be addressed to Kejun Wen; kejun.wen@jsums.edu

Received 28 August 2018; Revised 23 November 2018; Accepted 29 November 2018; Published 14 January 2019

Academic Editor: Hossein Moayedi



The unloading creep behavior of soft soil under lateral unloading stress path and excess pore water pressure is the core problem of time-dependent analysis of surrounding rock deformation under excavation of soft soil. The soft soil in Shenzhen, China, was selected in this study. The triaxial unloading creep tests of soft soil under different initial excess pore water pressures (0, 20, 40, and 60 kPa) were conducted with the $K_0$ consolidation and lateral unloading stress paths. The results show that the unloading creep of soft soil was divided into three stages: attenuation creep, constant velocity creep, and accelerated creep. The duration of creep failure is approximately 5 to 30 mins. The unloading creep behavior of soft soil is significantly affected by the deviatoric stress and time. The nonlinearity of unloading creep of soft soil is gradually enhanced with the increase of the deviatoric stress and time. The initial excess pore water pressure has an obvious weakening effect on the unloading creep of soft soil. Under the same deviatoric stress, the unloading creep of soft soil is more significant with the increase of initial excess pore water pressure. Under undrained conditions, the excess pore water pressure generally decreases during the lateral unloading process and drops sharply at the moment of unloading creep damage. The pore water pressure coefficients during the unloading process were 0.73–1.16, 0.26–1.08, and 0.35–0.96, respectively, corresponding to the initial excess pore water pressures of 20, 40, and 60 kPa.

## 1. Introduction

Soft soil is a kind of regional special soil with significant rheological characteristics and widely distributed in China's Pearl River Delta, Yangtze River Delta, and other coastal areas. The total area of the coastal zone is about 280,000 km$^2$, which is the most economically developed region in China. With the rapid development of economic construction, the abovementioned areas have carried out large-scale development of soft soil, such as soft soil deep foundation pits, underground shopping malls, and subway [1, 2]. The stress that soil body experienced is mainly an unloading process in the excavation of soft soil [3]. The engineering practice shows that the deformation, instability, and damage of the surrounding rock of soft soil do not occur immediately during the excavation or after the excavation, but they experience a period of history, that is, the unloading creep damage of soft soil occurs [4, 5]. Meanwhile, the high-level groundwater normally exists in soft soil areas, and the disturbance or vibration of construction will lead to large excess pore water pressure. The presence of pore water pressure will weaken the microstructure of the soft soil particles, and it can make the unloading creep damage of the soft soil extremely strong and even cause the rheological disasters. In 2003, Shanghai Metro Line 4 failed due to the freezing method, which caused the soft soil around the shield

tunnel to withstand high-pressure water and caused rheological disasters [6]. Therefore, the soft soil unloading mechanics caused by lateral unloading stress path and excess pore water pressure has become an inevitable problem in the design and construction of excavation of soft soil.

Studies have been conducted on different stress paths for soft soil since Lambe [7] proposed the concept of stress path. The early research on soft soil theory mainly focused on the strength and characteristics of soft soil under the loading stress path (e.g. AE loading stress path in Figure 1) [8]. With the deep understanding of the creep behaviors of soft soil, scholars have realized that the actual unloading stress path is neglected. The stresses and strains calculated by using parameters and models obtained from conventional axial loading tests (AE loading stress path in Figure 1) are found to be significantly different from the actual ones. However, the influence of the lateral unloading stress path on the creep behaviors of soft soil is neglected, which results in a theoretical difference between the theoretical calculation results and the actual stress and deformation. Therefore, selecting the stress path in accordance with the actual unloading process to explore the unloading creep behaviors of soft soil has attracted great attention from scholars and practical engineering.

Zhou and Chen [9] found that the creep effect of soil under lateral unloading conditions was significantly higher than that of axial loading through triaxial undrained tests on soft soil in the Pearl River Delta. Negative pore water pressure was generated when the soil sample was subjected to undrained shear under lateral unloading conditions. However, their study did not further study the variation law of negative pore water pressure. Fu et al. [10] conducted a triaxial lateral unloading creep test on soft soil in Shanghai, China. Their results showed that the creep of soft soil after unloading was divided into three stages: attenuation creep, constant velocity creep, and accelerated creep. During the creep process, the pore pressure coefficient changed with time. Zeng et al. [11] conducted a series of experiments on the mechanical properties of soft soil in Guangzhou at different consolidation conditions. Their results showed that the lateral unloading would increase shear stress and decrease volume stress, which could result in a dilatancy in the soil. The coefficient of pore water pressure was related to the consolidation state, but they did not study the variation law of pore water pressure coefficient.

The weakening effect of excess pore water pressure on soft soil in actual engineering is accompanied by the whole process of unloading creep of soft soil, which is very important to clarify the mechanism of unloading creep damage of soft soil. Li et al. [12] studied the changes of pore water pressure of clay subgrade in the process of dynamic vibration of construction and indicated that the dissipation time of excess pore water pressure in clay formation is 20–40 h. Zhu et al. [13] reported the pore water pressure caused by construction vibration in saturated soft soil area. They found that the distribution range of excess pore water pressure is around 43–64 kPa. Jian and Chang [14] analyzed the variation of soft soil strain and pore water pressure during the process of principal stress rotation. They found that shear

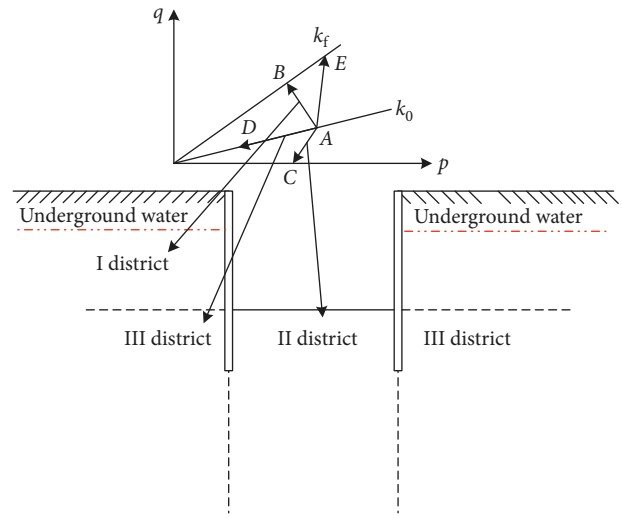


Figure 1: Schematic diagram of space excavation under soft soil.

stress has a significant impact on the accumulation of pore water pressure. Yan et al. [15] studied the variation of excess pore water pressure in saturated soft clay. The results showed that in the triaxial tensile test, the excess pore water pressure generated by the change of the deviatoric stress is positive. Cai et al. [16] studied the effect of consolidation stress paths on the shear characteristics of overconsolidated clay. They reported that the increase of the ratio of vertical and radial consolidation stress ($K$) could lead to lower negative excess pore water pressures.

Previous studies mainly focused on the unloading mechanical properties of soft soil under single lateral unloading path or the distribution of excess pore water pressure caused by construction vibration. The quantitative analysis of the unloading creep of soft soil under the coupling of lateral unloading stress path and excess pore water pressure is sparse. Therefore, this study considered the lateral unloading stress path and the excess pore water pressure caused by the construction in soft soil area in Shenzhen, China. A series of $K_0$ consolidation triaxial undrained unloading creep tests were carried out to investigate the effects of different initial excess pore water pressures, different consolidation confining pressures, and lateral unloading on the unloading creep behaviors of soft soil. This research would provide theoretical guidance for the excavation of soft soil and further lay the foundation for the future numerical simulation analysis of soft soil unloading creep.

## 2. Materials and Methods

*2.1. Soft Soil.* The test soils are taken from a soft soil foundation pit in Shenzhen. The soil is grayish black, smelly and contains a small amount of shells. In order to carry out sufficient contrast test, the lateral unloading strength test under different consolidation confining pressures and initial excess pore water pressures use disturbed soil samples. The natural density ($\rho$) and water content ($w$) of the soil sample are determined by the statistical average of the undisturbed soil. The above values are used as the expected values of the

disturbed soil samples. The cutting-ring density method is used to measure the natural density ($\rho$), the drying method to measure the water content ($w$), the pycnometer method to measure the soil specific gravity ($G_s$), the GYS-2 photoelectric liquid-plastic limit instrument to measure plastic limit, the TSZ automatic stress-controlled triaxial apparatus to measure the undrained cohesion ($c$), and the friction angle ($\varphi$) and the variable head method to measure the permeability coefficient $k$. Other properties of soft soils are determined by Geotechnical Test Method Standard (GBT50123-1999). The physicomechanical properties of soft soil are summarized in Table 1. The size of standard soil sample is 80.0 mm in height and 39.1 mm in diameter.

*2.2. Specimen Design.* To carry out the mechanical properties of soil unloading in accordance with engineering practice, the stress path involved in excavation must be firstly analyzed. The unloading path of space under soft soil (such as a foundation pit) can generally be simplified to three unloading stress paths as shown in Figure 1. The first is the AB stress path, which is the unloading path with only the lateral unloading of soil. The second is the AC stress path, which is the unloading path with the constant lateral load and the decrease of axial load. The third is the AD stress path, which is the unloading path with decreasing of both axial and lateral loads and accompanied by the rotation of the principal stress axis.

The AB unloading stress path involves analysis of lateral deformation and excavation stability of supporting structure. Therefore, this paper concentrated on the lateral unloading stress path (AB) in Zone I. According to study by Zhu et al. [13] and the actual construction of soft soil in Shenzhen, the excess pore water pressure of 17–64 kPa was monitored. Therefore, four different initial excess pore water pressures are proposed, which are $u_0 = 0$, 20, 40, and 60 kPa, respectively, to explore the unloading creep mechanical properties of soft soil under the coupling of excess pore water pressure and lateral unloading path.

The TSZ automatic stress control triaxial instrument is used in this study. The range of the axial pressure sensor is 1 kN; the range of the displacement sensor is 50 mm; the engineering range of the confining pressure is 1 MPa; the resolution is 1 kPa; the volume range of the back-pressure system is 120 $mm^3$; the volumetric accuracy is 1 $mm^3$.

*2.3. Experimental Procedure.* The back-pressure saturation system of TSZ automatic stress control triaxial apparatus is selected to saturate the soil sample. The 110 kPa confining pressure and 90 kPa back-pressure are applied, and the saturation of the soil can reach 98%. The three different consolidation confining pressures ($\sigma_3 = 100$, 200, and 300 kPa) are selected in this study. The unequal consolidation ($K_0 = 1 - \sin\varphi' = 0.53$) is used to restore the self-weight stress state of the soil. Therefore, the final axial pressures are 189, 377, and 566 kPa.

After the consolidation of the corresponding confining pressure $K_0$ is completed, the upper and lower drain valves of the triaxial apparatus are closed, and the initial excess pore water pressures $u_0 = 0$, 20, 40, and 60 kPa are applied to the interior soil through the back-pressure system. The lateral unloading creep test under undrained conditions is conducted in 6–7 stages. The unloading rate is $\Delta q = 1$ kPa/min. The duration of each stage after unloading is around 2–4 d, and the detailed unloading process is shown in Table 2. The confining pressure, axial pressure, axial deformation, and excess pore water pressure are recorded during the tests until axial strain reaches 15%.

## 3. Results and Discussion

*3.1. Study of Strain-Time Curve.* The unloading strain-time curves of soft soil under different initial excess pore water pressure with 100 kPa consolidation confining pressure are shown in Figure 2. The unloading strain-time curves of the confining pressure of 200 kPa and 300 kPa are similar to that of 100 kPa. They are not presented in this study. The deformation obtained from the triaxial creep test under the lateral unloading stress path can be divided into instantaneous deformation and unloading creep. The unloading creep of soft soil can be divided into three stages: attenuation creep, constant velocity creep, and failure creep. It can be seen that attenuated creep and failure creep occur mostly, and the constant creep happens only once in A5 unloading of Figure 2(c). Fu et al. [10] studied the unloading process of soft soil in Shanghai, China. They pointed out that constant creep would not occur during soft soil unloading creep, which is opposite to the results in this study. This could be due to that the loading time of each stage is too short in their study. Meanwhile, the unloading creep of soft soil is related to deviatoric stress ($q = \sigma_1 - \sigma_3$). In the case of A1 unloading in Figures 2(a)–2(c), when the deviatoric stress is low, it exhibits attenuated creep, and the amount of creep deformation is very small. In the case of A5 and A6 in Figure 2(a), when the deviatoric stress increases, the creep deformation of the soft soil becomes greater, and the time required to reach the stable condition is longer, but the stage is still in the attenuated creep stage. In the case of A7 in Figure 2(a), A6 in Figure 2(b), and A5 in Figure 2(d), when the deviatoric stress approaches the ultimate load, the creep deformation of the soft soil increases sharply within a few minutes until damage occurs, which is the failure creep.

The initial excess pore water pressure has an obvious weakening effect on the unloading creep of soft soil. Under the same consolidation confining pressure, the unloading creep deformation of the soft soil produced by the same deviatoric stress is greater while the initial excess pore water pressure increases. The higher initial excess pore water pressure is more likely to cause unloading creep damage. For example, in A4 unloading of Figures 2(a)–2(d), the creep deformation generated at the initial excess pore water pressures $u_0 = 0$, 20, 40, and 60 kPa are 0.33%, 2.41%, 5.14, and 9.74%, respectively. Therefore, the initial excess pore water pressure in soft soil should be reduced as much as possible to prevent unloading rheological damage in actual engineering.

Table 1: Physicomechanical properties of soft soil.

| Soil samples | Physical properties | | | | | | | | | Shear properties | |
|---|---|---|---|---|---|---|---|---|---|---|---|
| | $\rho$ (g/cm$^3$) | $w$ (%) | $e$ | $S_r$ (%) | $G_s$ | $w_L$ (%) | $w_P$ (%) | $I_P$ | $I_L$ | $c$ (kPa) | $\varphi$ (°) |
| Undisturbed sample* | 1.80 | 39.2 | 1.105 | 96.0 | 2.73 | 41.5 | 25.2 | 16.3 | 0.88 | 18.1 | 26.4 |
| Disturbed sample | 1.82 | 39.6 | 1.094 | 98.8 | | | | | | 19.9 | 28 |

*The average value of 30 undisturbed samples.

Table 2: The test unloading schemes.

| Unloading process | $\sigma_{3c}$ = 100 kPa | | $\sigma_{3c}$ = 200 kPa | | $\sigma_{3c}$ = 300 kPa | |
|---|---|---|---|---|---|---|
| | $\sigma_3$ (kPa) | $\sigma_1$ (kPa) | $\sigma_3$ (kPa) | $\sigma_1$ (kPa) | $\sigma_3$ (kPa) | $\sigma_1$ (kPa) |
| $K_0$ consolidation | 100 | 189 | 200 | 377 | 300 | 566 |
| A1 | 90 | 189 | 180 | 377 | 270 | 566 |
| A2 | 80 | 189 | 160 | 377 | 240 | 566 |
| A3 | 70 | 189 | 140 | 377 | 210 | 566 |
| A4 | 60 | 189 | 120 | 377 | 180 | 566 |
| A5 | 50 | 189 | 100 | 377 | 150 | 566 |
| A6 | 40 | 189 | 80 | 377 | 120 | 566 |
| A7 | 30 | 189 | — | — | — | — |

Under high initial excess pore water pressure, the soft soil can produce large creep deformation under low stress, which is beneficial to the discovery of unloading creep damage of soft soil in practical engineering. However, it is not easy to find unloading creep damage of soft soil under the low initial excess pore water pressure. For example, in Figures 2(a) and 2(b), the deformation of the soft soil after the first three stages of unloading is very small. With the accumulation of lateral unloading, the unloading creep of the soft soil gradually increases and eventually occurs unloading creep damage. The unloading creep damage of soft soil is more concealed and sudden under low initial excess pore water pressure. Therefore, during the actual unloading excavation process, the soft surrounding rock should be supported in time to prevent excessive lateral deformation and the soft soil unloading damage.

*3.2. Study of Deviatoric Stress-Strain Isochronal Curve.* It is incapable of studying the nonlinear creep properties of soft soil through strain-time curve. Zou et al. [17] and Dob et al. [18] reported that the creep of soft soil is nonlinear, and the linear creep only occurs at very lower stress. The lateral unloading creep deviatoric stress-strain curves of soft soil under different initial excess pore water pressures at consolidation confining pressure 100 kPa are shown in Figure 3. When the deviatoric stress is low, the curve can be approximately defined as a straight line, and the creep behaviors of soft soil exhibit linear viscoelastic properties. When the deviatoric stress is relatively high, the curve gradually changes from a straight line to a curve. The unloading creep characteristic exhibits strong nonlinear viscoplasticity, and the bending origin of the curve corresponds to the yield stress ($\sigma_s$) of the soft soil unloading creep. Wang et al. [19] reported a similar result in studying the creep behaviors of loess. Their study also indicated that the yield stress of loess is significantly higher than that of soft soil at confining pressure of 100 kPa.

The unloading creep behaviors of soft soil are not only related to the deviatoric stress, but also closely related to time. The tangent slope at any point of the curve is defined as the viscoelastic modulus of the creep curve ($E_{vel}$(t)). It can be seen from Figure 3 that at any deviatoric stress level, the $E_{vel}$(t) of soft soil creep decreases with time, especially at a higher level of deviatoric stress. It also indicates that the nonlinearity of soft soil unloading creep increases with time.

The initial excess pore water pressure also has a significant weakening effect on the yield stress ($\sigma_s$) of soft soil unloading creep. Table 3 shows the relationship between the initial excess pore water pressure and the yield stress ($\sigma_s$). It is found that the soft soil yield stress ($\sigma_s$) decreases linearly with the increase of the initial excess pore water pressure. Meanwhile, the slope of the fitting relationship tended to increase with the confining pressure, indicating that the effect of excess pore water pressure on the yield stress is greater at a high confining pressure.

*3.3. Change of Excess Pore Water Pressure.* The pore water pressure-time curve under different pore water pressures with 100 kPa consolidation confining pressure is shown in Figure 4. From the whole process of unloading creep behavior of soft soil, the excess pore water pressure generally shows a downward trend with the intensification of lateral unloading of soft soil. This is mainly due to the reduction of the lateral restraint of the soil and the dilatation of the soil. Especially when the creep failure of the soil sample is about to occur, the high stress can immediately cause excessive plastic shear deformation of the soil, and the excess pore water pressure will drop sharply. According to the principle of effective stress of Terzaghi, while the excess pore water pressure drops dramatically, the effective stress will suddenly increase, which may cause the unloading creep failure of the soil. Therefore, the excess pore water pressure should be closely monitored in actual engineering to prevent the creep failure of soil. Figure 5 showed the pore water pressure-time curve at initial excess

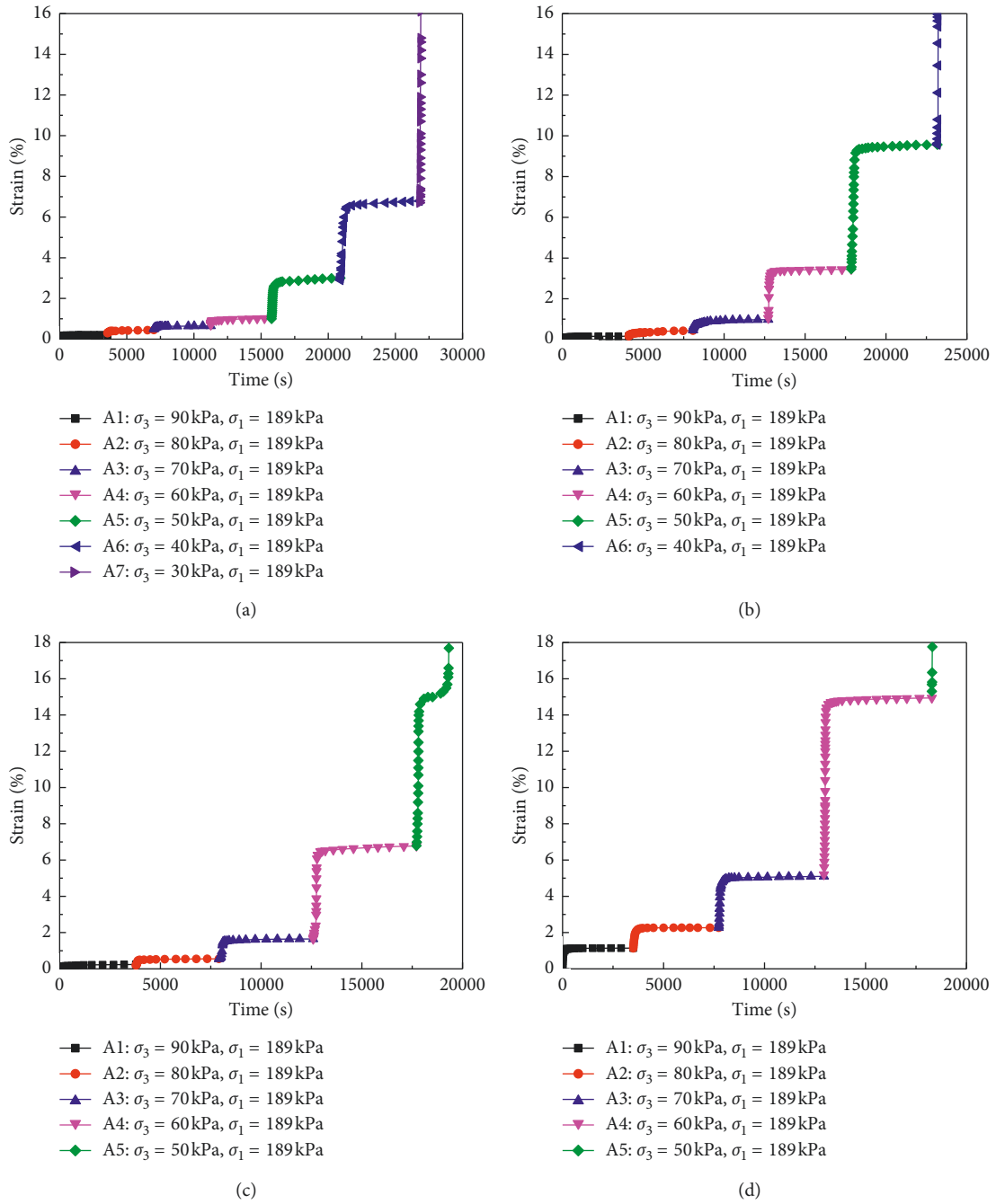


Figure 2: The unloading strain-time curves of soft soil under different initial excess pore water pressures (consolidation confining pressure 100 kPa). (a) Excess pore water pressure $u_0 = 0$ kPa. (b) Excess pore water pressure $u_0 = 20$ kPa. (c) Excess pore water pressure $u_0 = 40$ kPa. (d) Excess pore water pressure $u_0 = 60$ kPa.

pore water pressure (40 kPa). At the initial stage of each stage unloading, all excess pore water pressures suddenly drop. When they drop to the lowest value, the excess pore water pressure gradually rises and remains stable. The excess pore water pressure drops slightly in the A1–A3 level but drops sharply in the A4 and A5 levels. This is consistent with the results of creep deformation of soft soil in Figure 2(c). Therefore, when the soft soil unloading creep increases, the volumetric volume expansion of the soil will increase, resulting in an increase in excess pore water pressure.

The above changes in the excess pore water pressure are related to the unloading creep mechanism of soft soil. The unloading creep of soft soil actually is the process of damage and self-healing effect of the grain structure inside the soil. After the lateral unloading occurs, the force balance between the soil particles is broken, and the soil particles try to adjust the relative position to reach a new balance. When the self-healing effect of the soil is greater than the damage effect, the soil will enter the attenuated creep stage, the deformation tends to a stable value, and the excess water pressure will rise

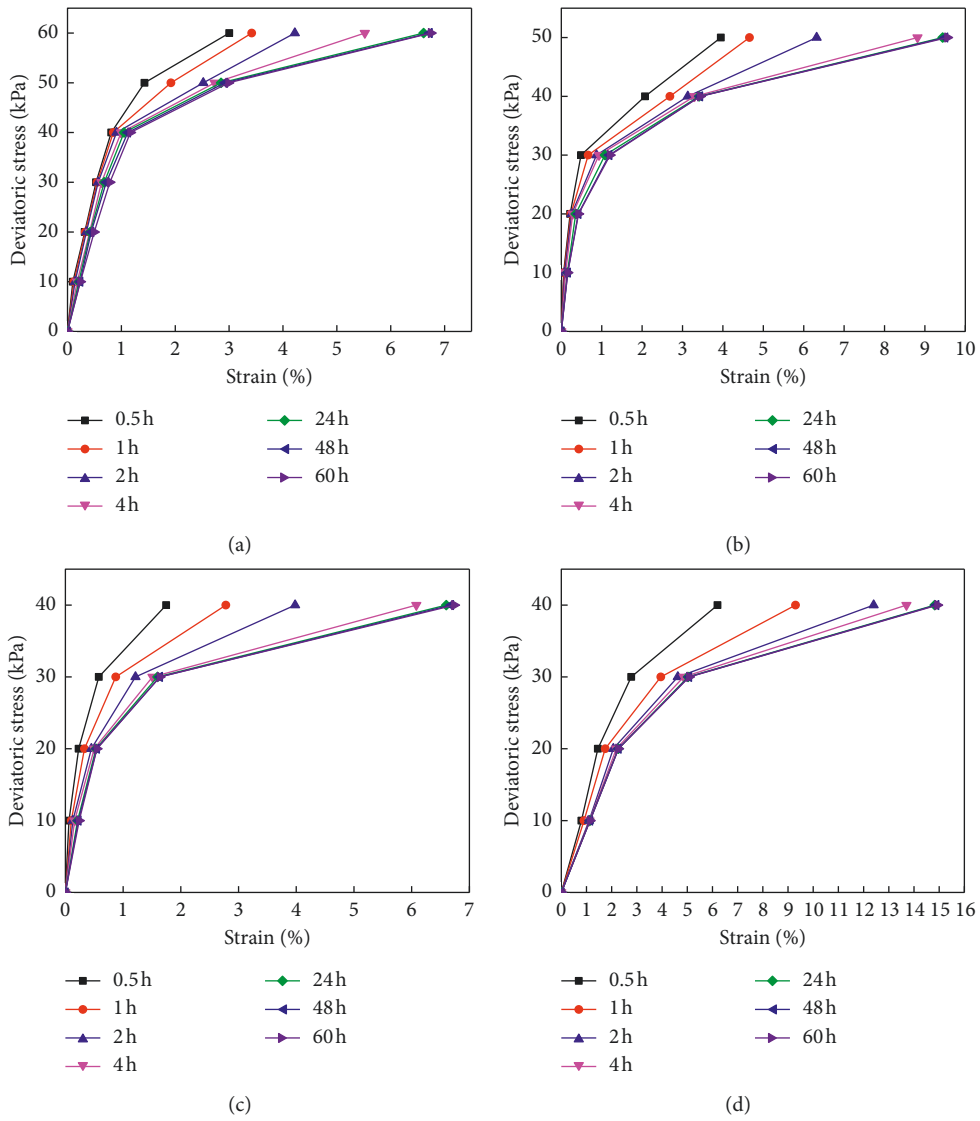


Figure 3: Unloading creep deviatoric stress-strain curves of soft soil under different initial excess pore water pressure (consolidation confining pressure 100 kPa). (a) Initial excess pore water pressure $u_0 = 0$ kPa. (b) Initial excess pore water pressure $u_0 = 20$ kPa. (c) Initial excess pore water pressure $u_0 = 40$ kPa. (d) Initial excess pore water pressure $u_0 = 60$ kPa.

Table 3: The fitting relationship between creep yield stress and initial pore water pressure.

| Consolidation confining pressure (kPa) | The relationship between $\sigma_s$ and $u$ | $R^2$ |
|---|---|---|
| 100 | $\sigma_s = -0.325u + 38.5$ | 0.9486 |
| 200 | $\sigma_s = -0.415u + 65.7$ | 0.9901 |
| 300 | $\sigma_s = -0.460u + 68.8$ | 0.9832 |

slightly. This process is particularly evident in the A1–A3 level where the initial excess pore water pressure is 40 and 60 kPa. When the damage effect is greater than the self-healing effect, the new balance can not be achieved by the adjustment of the soil particles. The plastic deformation caused by shearing will directly appear as a dilatancy phenomenon, resulting in a sharp decrease in the excess pore water pressure as shown in the A5 level of Figure 5.

Skempton [20] analyzed unloading problems of clay soil and defined the excess pore water pressure as $\Delta u = B[\Delta\sigma_3 + A(\Delta\sigma_1 - \Delta\sigma_3)]$. For saturated soft clay, $B$ is equal to 1. Therefore, the equation can be redefined as $\Delta u = \Delta\sigma_3 + A(\Delta\sigma_1 - \Delta\sigma_3)$, where $A$ is the pore pressure coefficient, $\sigma_1$ is the axial pressure, $\sigma_3$is the confining pressure, and $u$ is the excess pore water pressure. The relationship between pore water pressure coefficient and time is shown in Figure 6. It can be seen that the highest pore water pressure coefficient is found at excess pore water pressure (20 kPa) and the lowest at excess pore water pressure (60 kPa). Moreover, the pore water pressure

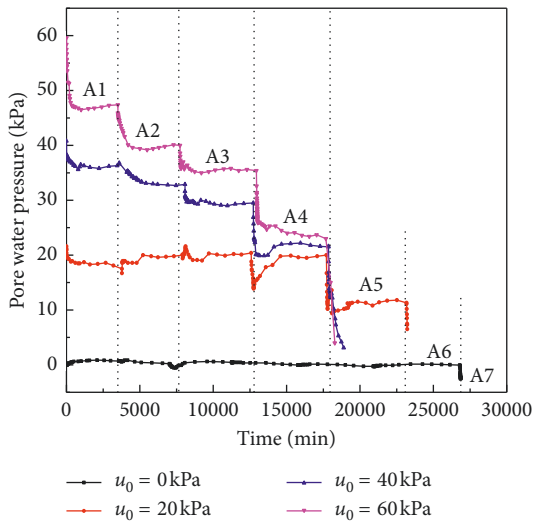


Figure 4: The pore water pressure-time curve at different pore water pressures.

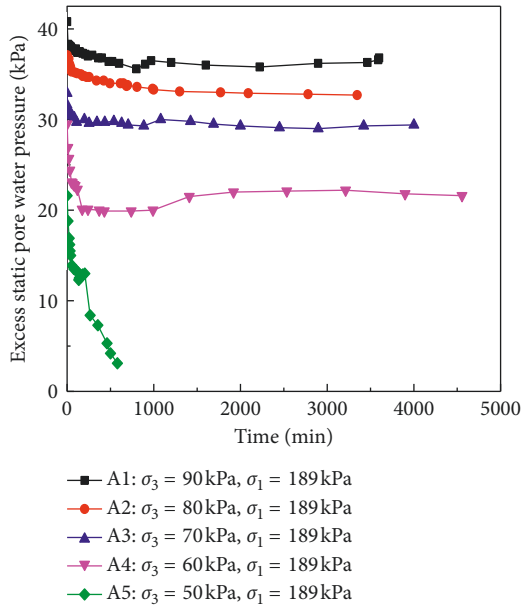


Figure 5: The pore water pressure-time curve at initial excess pore water pressure (40 kPa).

coefficients at initial excess pore water pressure 20, 40, and 60 kPa are approximate 0.73–1.16, 0.26–1.08, and −0.35–0.96, respectively. Fu et al. [10] reported the pore water pressure coefficients to be around 1.0–1.3. The coefficients found in this study are generally lower than the reported ones. This could be due to that the initial excess pore water pressure is not applied in their study.

*3.4. Influence of Consolidation Confining Pressure on Creep.* The creep deformation of soft soil under lateral unloading is not only related to axial stress and initial excess pore water pressure, but also closely related to the consolidation confining pressure of soft soil. The comparison of

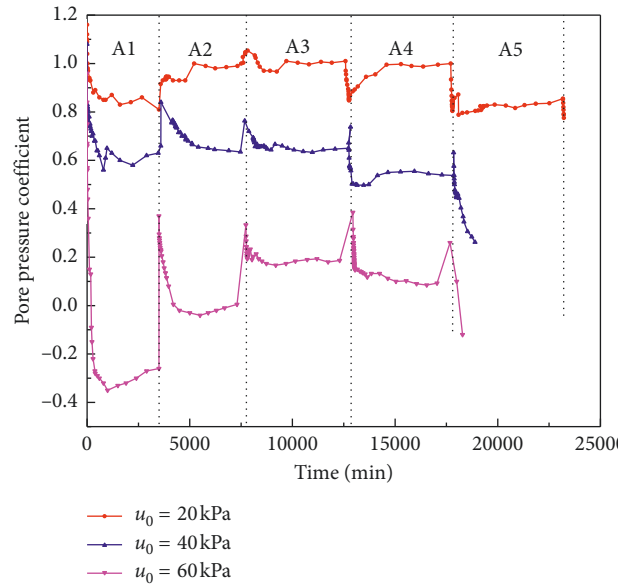


Figure 6: The relationship between pore water pressure coefficient and time.

axial strain at different confining pressures under the same axial unloading stress is summarized in Table 4. It can be seen that the higher excess pore water pressure can yield greater maximum strain at all consolidation confining pressures. Meanwhile, the maximum strain increases with the decrease of consolidation confining pressure under the same axial unloading stress with all initial pore water pressures. The greatest strain value happened at confining pressure (100 kPa) is approximately two orders of magnitude higher than that at confining pressure (300 kPa), indicating that the confining pressure has a great influence on the unloading and creeping behavior of soft soil. However, the higher confining pressure can contribute to consolidating the soft soil samples. Therefore, soft foundation treatment methods such as preloading and vacuum preloading can be implemented in advance to increase the degree of consolidation of soft soil during excavation of soft soil.

## 4. Conclusion

The undrained triaxial unloading creep tests of soft soil in Shenzhen, China, were conducted in this study. The effect of different initial excess pore water pressures and the lateral unloading stress path was also studied. The following can be concluded:

(1) The unloading creep curve of soft soil under the lateral unloading stress path is closely related to the deviatoric stress. With the increase of the deviatoric stress, the creep can be divided into attenuated creep, constant velocity creep, and failure creep stages. Meanwhile, the creep deformation is also related to the consolidation confining pressure. With the reduction of the confining pressure, the soft soil is more prone to have unloading creep.

Table 4: The comparison of axial strain at different confining pressures under the same axial unloading stress.

| Excess pore water pressure (kPa) | Axial unloading stress (40 kPa) | | $\varepsilon_{A4}/\varepsilon_{B2}$ | Axial unloading stress (60 kPa) | | $\varepsilon_{B3}/\varepsilon_{C2}$ |
|---|---|---|---|---|---|---|
| | $\sigma_{3c} = 100$ kPa A4 maximum strain ($\varepsilon_{A4}$) | $\sigma_{3c} = 200$ kPa B2 maximum strain ($\varepsilon_{B2}$) | | $\sigma_{3c} = 200$ kPa B3 maximum strain ($\varepsilon_{B3}$) | $\sigma_{3c} = 300$ kPa C2 maximum strain ($\varepsilon_{C2}$) | |
| 0 | 1.03 | 0.19 | 5.42 | 0.57 | 0.26 | 2.19 |
| 20 | 3.45 | 0.27 | 12.78 | 0.71 | 0.30 | 2.37 |
| 40 | 6.78 | 0.32 | 21.19 | 0.92 | 0.32 | 2.88 |
| 60 | 14.94 | 0.38 | 39.31 | 1.13 | 0.36 | 3.14 |

(2) The initial excess pore water pressure has an obvious weakening effect on the unloading creep of soft soil. Under the same deviatoric stress, the unloading creep deformation of soft soil becomes larger with the increase of initial excess pore water pressure.

(3) The unloading creep behaviors of soft soil are related to both deviatoric stress and time: when the deviatoric stress is lower than the yield stress, the deviatoric stress-strain curve exhibits linear viscoelastic properties. When the deviatoric stress is higher than the yield stress, it exhibits strong nonlinear viscoplastic properties. Meanwhile, the nonlinearity of unloading creep is gradually enhanced with the increase of time.

(4) Under undrained conditions, the excess pore water pressure drops slightly in the early stage but drops sharply in the failure creep stage. Also, the pore water pressure coefficient decreases with the increase of the initial excess pore water pressure.

## Data Availability

All the data supporting the conclusions of this study are presented in the tables of the manuscript. All data are available upon request from the corresponding author (kejun.wen@jsums.edu).

## Conflicts of Interest

The authors declare that they have no conflicts of interest.

## Acknowledgments

This paper is based on the work supported by the Scientific and Technological Research Program of Chongqing Municipal Education Commission (Nos. KJ1713327 and KJ1600532), China Scholarship Council Program (No. 201708505131), Chongqing University of Science and Technology Research Program (No. ck2017zkyb013), School of Civil Engineering and Architecture (Grant No. JG201703) from Chongqing University of Science and Technology, and Chongqing Research Program of Basic Research and Frontier Technology by Chongqing Science and Technology Commission (No. cstc2015jcyjA90012).

## References

[1] R. Chen, F. Meng, Z. Li, Y. Ye, and J. Ye, "Investigation of response of metro tunnels due to adjacent large excavation and protective measures in soft soils," *Tunnelling and Underground Space Technology*, vol. 58, pp. 224–235, 2016.

[2] Z. Zhang, M. Huang, and W. Wang, "Evaluation of deformation response for adjacent tunnels due to soil unloading in excavation engineering," *Tunnelling and Underground Space Technology*, vol. 38, pp. 244–253, 2013.

[3] R. P. Chen, Z. C. Li, Y. M. Chen, C. Y. Ou, Q. Hu, and M. Rao, "Failure investigation at a collapsed deep excavation in very sensitive organic soft clay," *Journal of Performance of Constructed Facilities*, vol. 29, no. 3, article 04014078, 2013.

[4] M. Wang, "Tunneling by TBM/shield in China: state-of-art, problems and proposals," *Tunnel Construction*, vol. 34, no. 3, pp. 179–187, 2014.

[5] G. B. Liu and X. Y. Hou, "Unloading stress-strain characteristic for soft clay," *Underground Engineering and Tunnels*, vol. 2, pp. 16–23, 1997.

[6] Q. H. Qian and X. L. Rong, "State, issues and relevant recommendations for security risk management of China's underground engineering," *Chinese Journal of Rock Mechanics and Engineering*, vol. 27, no. 4, pp. 649–655, 2008.

[7] T. W. Lambe, "Stress path method," *Journal of the Soil Mechanics and Foundations Division*, vol. 93, no. 6, pp. 268–277, 1967.

[8] A. Negahdar, S. Yadegari, and S. Houshmandi, "Investigation of parameters affecting creep behavior of sandy clay soil in laboratory conditions," *Jordan Journal of Civil Engineering*, vol. 11, no. 1, pp. 80–90, 2017.

[9] Q. J. Zhou and X. P. Chen, "Test research on typical mechanical characteristics of soft clay under lateral unloading condition," *Chinese Journal of Rock Mechanics and Engineering*, vol. 28, no. 11, pp. 2215–2221, 2009.

[10] Y. B. Fu, H. H. Zhu, and J. Yang, "Experimental study of time dependent properties and pore water pressure of soft clay under unloading," *Chinese Journal of Rock Mechanics and Engineering*, vol. 28, no. 1, pp. 3244–3249, 2009.

[11] L. L. Zeng and X. P. Chen, "Analysis of mechanical characteristics of soft soil under different stress paths," *Rock and Soil Mechanics*, vol. 30, no. 5, pp. 1264–1270, 2009.

[12] X. J. Li, S. C. Li, K. Yao, S. C. Zhu, and G. R. Lv, "Experiment study of excess pore water pressure change during dynamic compaction of huangfan district," *Rock and Soil Mechanics*, vol. 232, no. 9, pp. 2815–2820, 2011.

[13] X. R. Zhu, Y. H. He, C. F. Xu, and Z. L. Wang, "Excess pore water pressure caused by single pile driving in saturated soft soil," *Chinese Journal of Rock Mechanics and Engineering*, vol. 24, pp. 5740–5744, 2005.

[14] Z. Jian and X. Changjie, "Impact of shear stress on strain and pore water pressure behavior of intact soft clay under principal stress rotation," *Geotechnical Testing Journal*, vol. 37, no. 3, pp. 447–462, 2014.

[15] S. W. Yan, J. J. Zhang, Y. H. Tian, and L. Q. Sun, "Pore pressure characteristics in isotropic consolidated saturated

clay under unloading conditions," *Journal of Marine Science and Technology*, vol. 24, no. 1, pp. 19–25, 2016.

[16] Y. Cai, B. Hao, C. Gu, J. Wang, and L. Pan, "Effect of anisotropic consolidation stress paths on the undrained shear behavior of reconstituted Wenzhou clay," *Engineering Geology*, vol. 242, pp. 23–33, 2018.

[17] C. Zou, Y. Wang, J. Lin, and Y. Chen, "Creep behaviors and constitutive model for high density polyethylene geogrid and its application to reinforced soil retaining wall on soft soil foundation," *Construction and Building Materials*, vol. 114, pp. 763–771, 2016.

[18] H. Dob, S. Messast, M. Boulon, and E. Flavigny, "Treatment of the high number of cycles as a pseudo-cyclic creep by analogy with the soft soil creep model," *Geotechnical and Geological Engineering*, vol. 34, no. 6, pp. 1985–1993, 2016.

[19] P. C. Wang, Y. H. Luo, L. X. Hu, and S. J. Wang, "Research on triaxial creep characteristics and model of remolded loess," *Rock and Soil Mechanics*, vol. 36, no. 6, pp. 1627–1632, 2015.

[20] A. W. Skempton, "The pore-pressure coefficients A and B," *Géotechnique*, vol. 4, no. 4, pp. 143–147, 1954.